Advances in Radiation Oncology (2023) 8, 101137

advances in radiation oncology

www.advancesradonc.org

Scientific Article

Radiation Therapy Modulates Tumor Physical Characteristics to Reduce Intratumoral Pressure and Enhance Intratumoral Drug Delivery and Retention

Hampartsoum B. Barsoumian, PhD,[a,1] Rahul A. Sheth, MD,[b,1] Rishab Ramapriyan, BS,[a] Ethan Hsu, BS,[a] Mihai Gagea, DVM,[c] Kaitlyn Crowley, BS,[a] Duygu Sezen, MD,[a,d] Malea Williams, BS,[b] and James W. Welsh, MD[a,*]

[a]Department of Radiation Oncology, The University of Texas MD Anderson Cancer Center, Houston, Texas; [b]Department of Interventional Radiology, The University of Texas MD Anderson Cancer Center, Houston, Texas; [c]Department of Veterinary Medicine and Surgery, The University of Texas MD Anderson Cancer Center, Houston, Texas; and [d]Department of Radiation Oncology, Koc University School of Medicine, Istanbul, Turkey

Received 11 October 2022; accepted 27 November 2022

Abstract

Purpose: High intratumoral pressure, caused by tumor cell-to-cell interactions, interstitial fluid pressure, and surrounding stromal composition, plays a substantial role in resistance to intratumoral drug delivery and distribution. Radiation therapy (XRT) is commonly administered in conjunction with different intratumoral drugs, but assessing how radiation can reduce pressure locally and help intratumoral drug administration and retention is important.

Methods and Materials: 344SQ-parental or 344SQ-anti-programmed cell death protein 1-resistant lung adenocarcinoma cells were established in 129Sv/Ev mice, and irradiated with either 1 Gy × 2, 5 Gy × 3, 8 Gy × 3, 12 Gy × 3, or 20 Gy × 1. Intratumoral pressure was measured every 3 to 4 days after XRT. Contrast dye was injected into the tumors 3- and 6-days after XRT, and imaged to measure drug retention.

Sources of support: Bristol Myers Squibb funded this work.

Disclosures: Dr Welsh reports research support from GlaxoSmithKline, Bristol Meyers Squibb, Merck, Nanobiotix, RefleXion, Alkermes, Artidis, Mavu Pharma, Takeda, Varian, Checkmate Pharmaceuticals, and HotSpot Therapeutics. Dr Welsh also serves/served on the scientific advisory board for Legion Health care Partners, RefleXion Medical, MolecularMatch, Merck, AstraZeneca, Aileron Therapeutics, OncoResponse, Checkmate Pharmaceuticals, Mavu Pharma, Alpine Immune Sciences, Ventana Medical Systems, Nanobiotix, China Medical Tribune, GI Innovation, Genentech, and Nanorobotix, as well as serves as consultant for Lifescience Dynamics Limited. In addition, Dr Welsh has/had speaking engagements for Ventana Medical Systems, US Oncology, Alkermes, Boehringer Ingelheim, Accuray, and RSS; holds/held stock or ownership in Alpine Immune Sciences, Checkmate Pharmaceuticals, Healios, Mavu Pharma, Legion Health care Partners, MolecularMatch, Nanorobotix, OncoResponse, and RefleXion; and has accepted honoraria in the form of travel costs from Nanobiotix, RefleXion, Varian, Shandong University, The Korea Society of Radiology, Aileron Therapeutics, and Ventana. Moreover, Dr Welsh has the following patents: MP470 (amuvatinib), MRX34 regulation of PDL1, XRT technique to overcome immune resistance, and Radiotherapies and uses thereof. MD Anderson Cancer Center has a trademark for RadScopal. Dr Barsoumian has a patent for Radiotherapies and uses thereof. Dr Sheth is a Consultant for Replimune, StarPAX, Boston Scientific, Medtronic, and TriSalus. All other authors have no disclosures to declare.

Data sharing statement: All data generated and analyzed during this study are included in this published article (and its supplementary material files). Further inquiries can be directed to the corresponding author.

[1] H.B.B. and R.A.S. contributed equally to this work.

*Corresponding author: James W. Welsh, MD; E-mail: jwelsh@mdanderson.org

https://doi.org/10.1016/j.adro.2022.101137

Results: In the 344SQ-parental model, low-dose radiation (1 Gy × 2) created an early window of reduced intratumoral pressure 1 to 3 days after XRT compared with untreated control. High-dose stereotactic radiation (12 Gy × 3) reduced intratumoral pressure 3 to 12 days after XRT, and 20 Gy × 1 showed a delayed pressure reduction on day 12. Intermediate doses of radiation did not significantly affect intratumoral pressure. In the more aggressive 344SQ-anti-programmed cell death protein 1-resistant model, low-dose radiation reduced pressure 1 to 5 days after XRT, and 12 Gy × 3 reduced pressure 1 to 3 days after XRT. Moreover, both 1 Gy × 2 and 12 Gy × 3 significantly improved drug retention 3 days after XRT; however, there was no significance detected 6 days after XRT. Lastly, a histopathologic evaluation showed that 1 Gy × 2 reduced collagen deposition within the tumor, and 12 Gy × 3 led to more necrotic core and higher extracellular matrix formation in the tumor periphery.

Conclusions: Optimized low-dose XRT, as well as higher stereotactic XRT regimen led to a reduction in intratumoral pressure and increased drug retention. The findings from this work can be readily translated into the clinic to enhance intratumoral injections of various anticancer agents.

Introduction

Medical advances over the past years have elucidated and refined the concept of using immunotherapy in solid tumors. There is a growing number of clinical trials using immunotherapy in conjunction with chemotherapy and radiation therapy (XRT), emphasizing the concept that combining immunotherapy with other treatment modalities may be critical to achieve robust antitumor responses.[1,2] Shedding light on radiation-based combinations is particularly critical because XRT may prime antitumor immunity and reduce intratumoral pressure, the latter of which is the primary focus of this study.[3-6] The rationale and importance of reducing intratumoral/intraoncotic pressure by XRT stem from the need to enhance intratumoral drug delivery and retention. Currently, 24 of 130 clinical studies investigating immune modulating therapies involve intratumoral routes of administration.[7-11] The benefits of doing so include avoiding off-target toxicity, using a lower and less toxic drug dose, and priming local T cells for immune response.[12,13]

Developments in image guided local drug injection techniques are growing fast. However, elevated intratumoral pressure presents a barrier because the pressure differential between the center and outer regions of solid tumors can cause hypoxia, increase metastatic potential, and compromise successful intratumoral drug delivery.[14,15] Although the mechanisms are not entirely understood, elevated tumor interstitial or intratumoral pressure can be attributed to blood-vessel leakiness, lymph vessel abnormalities, interstitial fibrosis, modified interstitial matrix, and tumor cells proliferating within a confined space.[15]

To address this issue, we propose the use of XRT to reduce the pressure-induced convection force that opposes the diffusion of therapeutic agents injected intratumorally. Cancer cells with their inhibitory stroma produce cytokines, such as transforming growth factor beta (TGF-β), which further contribute to abnormal vasculature and thus elevate intratumoral pressure.[15] We recently showed that low-dose radiation therapy can, in fact, reduce TGF-β levels locally and modulate the tumor microenvironment (TME).[16] Beyond reducing intratumoral pressure, XRT has also been shown to reoxygenate certain portions of irradiated tumors and increase pO_2 levels, hence increasing tumor treatability by overcoming hypoxia.[17]

Although certain physical and cellular attributes contributing to intratumoral pressure are well understood, many aspects remain that warrant further research, especially in the context of XRT.[18,19] In this paper, we seek to optimize the radiation dose and fractionation schedule to find the best window for intratumoral drug delivery. To our knowledge, this is the first study to comprehensively explore how to use radiation to decrease intratumoral pressure, thereby increasing the success of intratumoral drug delivery into solid tumors.

Methods and Materials

Mice and tumor establishment

All animal protocols were reviewed and approved by the Institutional Animal Care and Use Committee of the University of Texas MD Anderson Cancer Center. 344SQ-parental (344SQ-P) or 344SQ-anti-programmed cell death protein 1-resistant (344SQ-R) lung adenocarcinoma cells were subcutaneously implanted on day 0 in the hind legs of 8- to 12-week old 129Sv/Ev mice, at a dose of 5×10^5 cells for parental and 0.5×10^5 for resistant. When tumors reached 7 to 8 mm in diameter, they were locally irradiated using a Cesium source. The radiation doses tested were 1 Gy × 2, 5 Gy × 3, 8 Gy × 3, 12 Gy × 3, and 20 Gy × 1. The different fractions were scheduled such that all treatments were completed on day 10 after tumor inoculation. Intratumoral pressure was recorded using a pressure transducer (Compass CT) at various timepoints (days 11, 13, 18, 22, 27, and 33), and measurements were graphed accordingly. Tumor growth was also recorded twice per week using digital calipers, and the mice were euthanized when the tumor reached 14 mm in diameter.

In vivo evaluation of percutaneous intratumoral delivery and retention

344SQ-P tumors were established in 129Sv/Ev mice. XRT was delivered on day 7 to the experimental groups as follows: Untreated control (Ctrl), 1 Gy × 2, 5 Gy × 3, 8 Gy × 3, 12 Gy × 3, and 20 Gy × 1. Intratumoral drug delivery deposition and retention were evaluated by advancing a 25-gauge needle into the tumor under ultrasound visualization (Siemens Acuson). Ultrasound imaging guidance was used to ensure accurate positioning of the needle within the lesion. Next, 100 uL of an iodinated contrast agent (Visipaque 320) was delivered via the 25-gauge needle into the tumor under live fluoroscopic imaging (Siemens Artis-Q). To standardize the injection rate, the injections were performed using a syringe pump (Harvard Apparatus) at a rate of 5 cc per minute. The Siemens Artis Q C-Arm was run at 7.5 frames per second to monitor the injections.

The procedures were performed by an interventional radiologist with 7 years of experience with preclinical and clinical intratumoral injection procedures. Animals were immediately scanned with microCT imaging with 100 micron resolution (Bruker SkyScan). The volumetric images were analyzed with a 3-dimensional image analysis software program (MIM Maestro) by a radiologist with 10 years of volumetric imaging analysis. The tumor volume, as well as the volume of distribution of the injected contrast agent, were calculated. The percent contrast agent retention was calculated by dividing contrast volume by tumor volume, multiplied by 100 to obtain percentage tumor fill.

Tumors histopathologic evaluation

344SQ-P tumor cells were subcutaneously injected in 129Sv/Ev mice on day 0. When tumors reached 7 to 8 mm in diameter, low-dose XRT (1 Gy × 2) was given on days 7 and 8, and high-dose XRT (12 Gy × 3) was given on days 7, 8, and 9. Low-dose tumors were harvested on day 10 and high-dose tumors on day 13. The mice were euthanized, and the tumors were dissected and fixed with 10% neutral buffered formalin solution. Formalin fixed tumors were cut in half through the middle on the larger diameter plan, and the largest cut surfaces were obtained, processed, and embedded into paraffin blocks.

From the paraffin blocks, 4-μm thick sections of tumor tissues were cut and mounted on glass slides, and then stained with hematoxylin and eosin and Masson's trichrome stains per the methods in the book *Histotechnology: A Self-Instructional Text.*[20] The stained slides were examined with an Olympus BX41 microscope, and then scanned with an Aperio Scanscope AT2. For the quantification of extracellular collagen stained with the Masson's trichrome method, we used Aperio image analysis algorithms.

Results

Optimized radiation dosing reduces intratumoral pressure in 344SQ-parental lung adenocarcinoma model

To test the effect of radiation on intratumoral pressure, 0.5×10^6 344SQ-P lung adenocarcinoma cells were inoculated into the right hind legs of 129Sv/Ev mice on day 0. Additionally, the primary tumor growth measurements were monitored throughout the 35-day observation period (Fig. 1A). Compared with the Ctrl group, all experimental groups showed increased antitumor responses (Ctrl vs 1 Gy × 2: $P < .0001$; Ctrl vs 5 Gy × 3: $P < .0001$; Ctrl vs 8 Gy × 3: $P < .0001$; Ctrl vs 12 Gy × 3: $P < .0001$; Ctrl vs 20 Gy × 1: $P < .0001$). Furthermore, 12 Gy × 3 controlled tumor growth better than 8 Gy × 3 ($P < .0001$). Tumors that were irradiated with 1 Gy × 2 and 12 Gy × 3 responded similarly, and were not significantly different ($P = .0827$). Optimized doses of radiation, including both low-dose (1 Gy × 2) and high-dose (12 Gy × 3 and 20 Gy × 1) XRT, reduced intratumoral pressure levels during the measurement period (1-12 days after XRT), but the intermediate doses of radiation (5 Gy × 3 and 8 Gy × 3) did not show any significant reduction in intratumoral pressure (Fig. 1B).

A multiple unpaired *t* test was conducted to compare the mean intratumoral pressure from different doses of radiation against the Ctrl at each timepoint. Low-dose XRT showed an early window of low intratumoral pressure 1 and 3 days after XRT. On day 1, there was a significant drop in pressure from 104.8 mm Hg in the Ctrl group to 67 mm Hg in the 1 Gy × 2 group ($P = .0543$). On day 3, the group that received 2 fractions of 1 Gy had a mean intratumoral pressure of 69.6 mm Hg versus 111.4 mm Hg in the Ctrl group ($P = .0591$). The tumors irradiated with 3 fractions of 12 Gy showed a delayed window of reduced intratumoral pressure 3, 8, and 12 days after XRT ($P = .0105$, $P = .040$, and $P = .013$ respectively). On the contrary, tumors irradiated with a single fraction of 20 Gy showed reduced pressure 1 and 12 days after XRT ($P = .0457$ and $P = .009$, respectively).

To check if there was any correlation between tumor size and intratumoral pressure at the first and last measurements taken for each group, we calculated the slope of the linear regression (Fig. E1A). In general, there was an upward trend for the Ctrl, as well as the radiation-treated groups, with an increase in tumor size.

Optimized radiation dosing reduces intratumoral pressure at varying timepoints in 344SQ-resistant lung adenocarcinoma model

To further examine the effect of radiation on intratumoral pressure, the same experimental design was used from

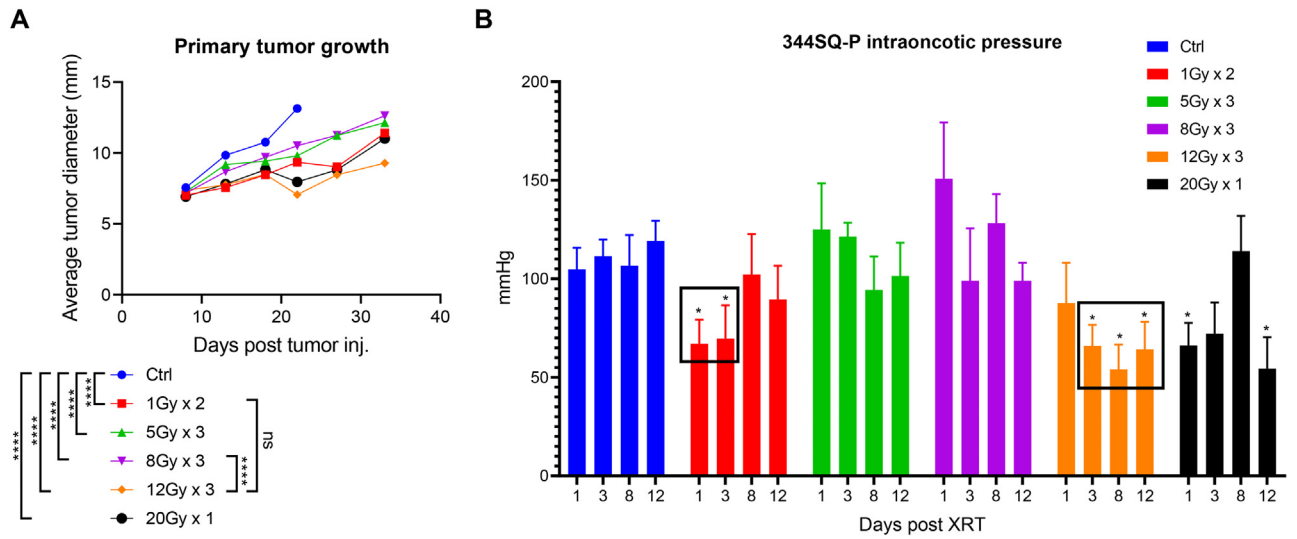

Figure 1 Optimized doses of radiation reduced intratumoral pressure in the 344SQ-parental model. A, Tumors were monitored throughout the measurement period to ensure that radiation started once the tumors reached 7 to 8 mm. Measurements were also used to confirm that tumors did not grow past 15 mm in diameter. B, Intratumoral pressure was measured 1, 3, 8, and 12 days after the last fraction of radiation therapy, and multiple *t* tests were conducted to analyze the difference in intratumoral pressure at each timepoint. $P \leq 0.05$ was considered significant. $^{*}P \leq 0.05$, $^{**}P \leq 0.01$, $^{***}P \leq 0.001$, $^{****}P \leq 0.0001$.

Figure 1, except that a different cancer cell line was used. Instead of using the 344SQ-P lung adenocarcinoma cell line, the more aggressive 344SQ-R cancer cell line was injected. The primary tumor growth measurements were monitored over the 40 days observation period (Fig. 2A). All experimental groups controlled tumor growth better than the Ctrl group (Ctrl vs 1 Gy × 2: $P = .0081$; Ctrl vs 5 Gy × 3: $P < .0001$; Ctrl vs 8 Gy × 3: $P < .0001$; Ctrl vs 12 Gy × 3: $P < .0001$; Ctrl vs 20 Gy × 1: $P < .0001$). There was no statistical difference in tumor growth between the group that received 8

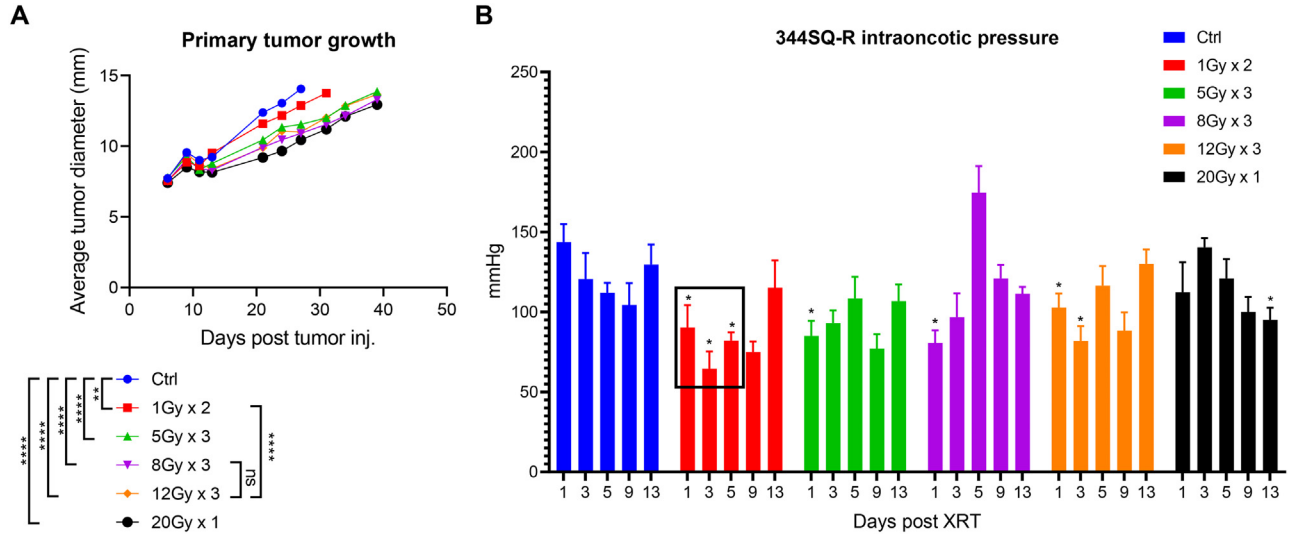

Figure 2 Different doses of radiation reduce intratumoral pressure at varying timepoints in the 344SQ-anti-programmed cell death protein 1-resistant model. A, The primary tumor was measured beginning on day 7 to ensure that tumors were ready to be irradiated, then measured twice per week to confirm that the tumor did not surpass 15 mm in diameter. B, Intratumoral pressure was measured 1, 3, 5, 9, and 13 days after radiation therapy, and multiple *t* tests were used to analyze the difference in intratumoral pressure at each timepoint. $P \leq 0.05$ was considered significant. $^{*}P \leq 0.05$, $^{**}P \leq 0.01$, $^{***}P \leq 0.001$, $^{****}P \leq 0.0001$.

Gy × 3 and 12 Gy × 3 (P = .1566). Additionally, 12 Gy × 3 hampered tumor growth better than 1 Gy × 2 (P = .0001).

All doses of radiation produced a different window of reduced intratumoral pressure (Fig. 2B), with 1 Gy × 2 producing the most statistical significance. Similar to the previous experiment using the 344SQ-P model, low-dose XRT created an early window of decreased intratumoral pressure 1, 3, and 5 days after the last fraction of XRT (P = .0175, P = .0209, P = .006, respectively). The 5 Gy × 3 and 8 Gy × 3 experimental groups only reduced pressure 1 day after XRT (P = .0038 and P = .0017, respectively). In addition, 12 Gy × 3 reduced intratumoral pressure 1 day after XRT (P = .0203), and had a strong trend of decreasing pressure on day 3 (P = .073). Contrary to the previous groups, 20 Gy × 1 only had a late effect on intratumoral pressure 13 days after XRT (P = .047).

To check if there was any correlation between tumor size and intratumoral pressure at the first and last measurement points for each group, we calculated the slope of the linear regression (Fig. E1B). As the tumor size increased, pressure decreased in the Ctrl group, showing that the 344SQ-R model tends to become less stiff by size increase, a characteristic of highly metastatic/soft tumors. An opposite trend was noticed in the irradiated groups with the exception of 20 Gy × 1, which favors high necrosis.

Optimized radiation dosing (1 Gy × 2 and 12 Gy × 3) enhances tumor fill and drug retention at different timepoints

To examine the effects of reduced intratumoral pressure on drug delivery and retention, the irradiated mice with 344SQ-P tumors were imaged 3 and 6 days after XRT (Figs. 3A and B). Three days after XRT (Fig. 3C), the mice that received 2 fractions of 1 Gy radiation had a significant increase in tumor fill of intratumorally injected iodinated contrast dye with a mean of 14.07% versus the Ctrl group

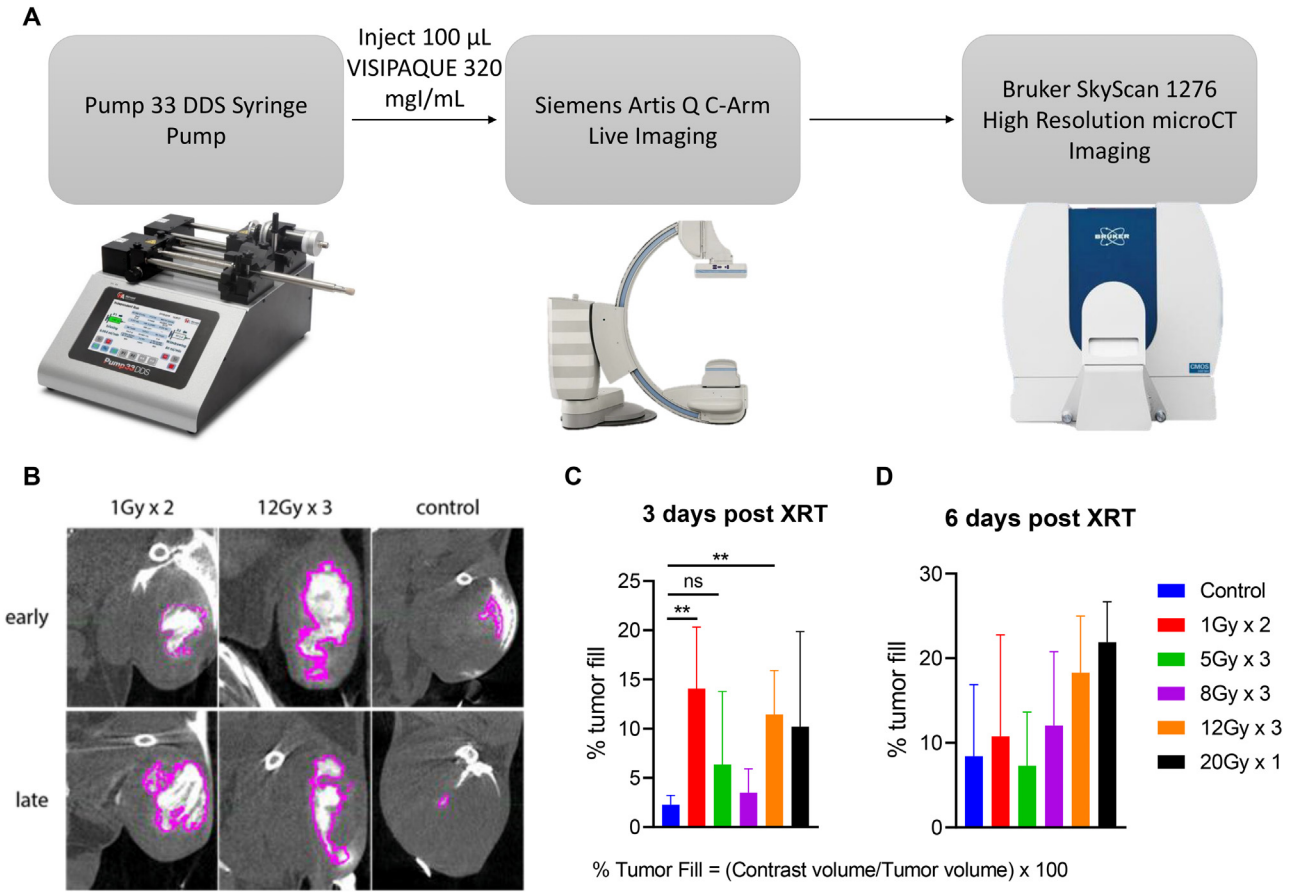

Figure 3 Optimized radiation dosing increases tumor fill and drug retention at different time frames in the 344SQ-parental model. A, Workflow for acquiring data and images regarding tumor fill 3 and 6 days after radiation therapy. B, Representative snapshots of live C-Arm imaging depicting optimal tumor fill of contrast dye with 1 Gy × 2 and 12 Gy × 3 radiation doses, while detecting a subcutaneous leak in the control group due to intratumoral pressure. Percent tumor fill was calculated by dividing contrast volume by tumor volume multiplied by 100. C, Percent tumor fill graphed for 3 days after radiation therapy. D, Percent tumor fill graphed for 6 days after radiation therapy. $P \leq 0.05$ was considered significant.

(2.29%; P = .008). Mice that were irradiated with 3 fractions of 12 Gy also showed a significant increase in tumor fill (11.45%) compared with the Ctrl group (P = .005). There was no significant increase in percent tumor fill 6 days after XRT (Fig. 3D); however, there was a strong increasing trend for the group that received 1 fraction of 20 Gy versus the Ctrl group (21.89% vs 8.43%; P = .058).

Low-dose radiation (1 Gy × 2) downregulates extracellular matrix and high-dose radiation (12 Gy × 3) upregulates peripheral extracellular matrix in 344SQ-P tumors

To fully understand how intratumoral pressure is reduced, immunohistochemistry was performed on 3 groups: Ctrl, 1 Gy × 2, and 12 Gy × 3. Masson's trichrome staining was used to visualize collagen and extracellular matrix (ECM; blue), nuclei (dark brown spots), muscle (red), and cytoplasm (pink). Afterward, the histochemical images were analyzed using the Aperio color deconvolution algorithm to measure the percentage of ECM present in the samples (Fig. 4A). The positive areas were shaded yellow to red depending on the intensity of the collagen stain, and the negative areas were shaded blue (Fig. 4B). Based on the values obtained from the algorithm, 2 fractions of 1 Gy XRT significantly lowered the percentage of ECM present (P = .037). Contrarily, 3 fractions of 12 Gy XRT significantly increased the percentage of ECM present (P = .05). However, high-dose radiation possibly reduced the intratumoral pressure from the direct killing of tumor cells.

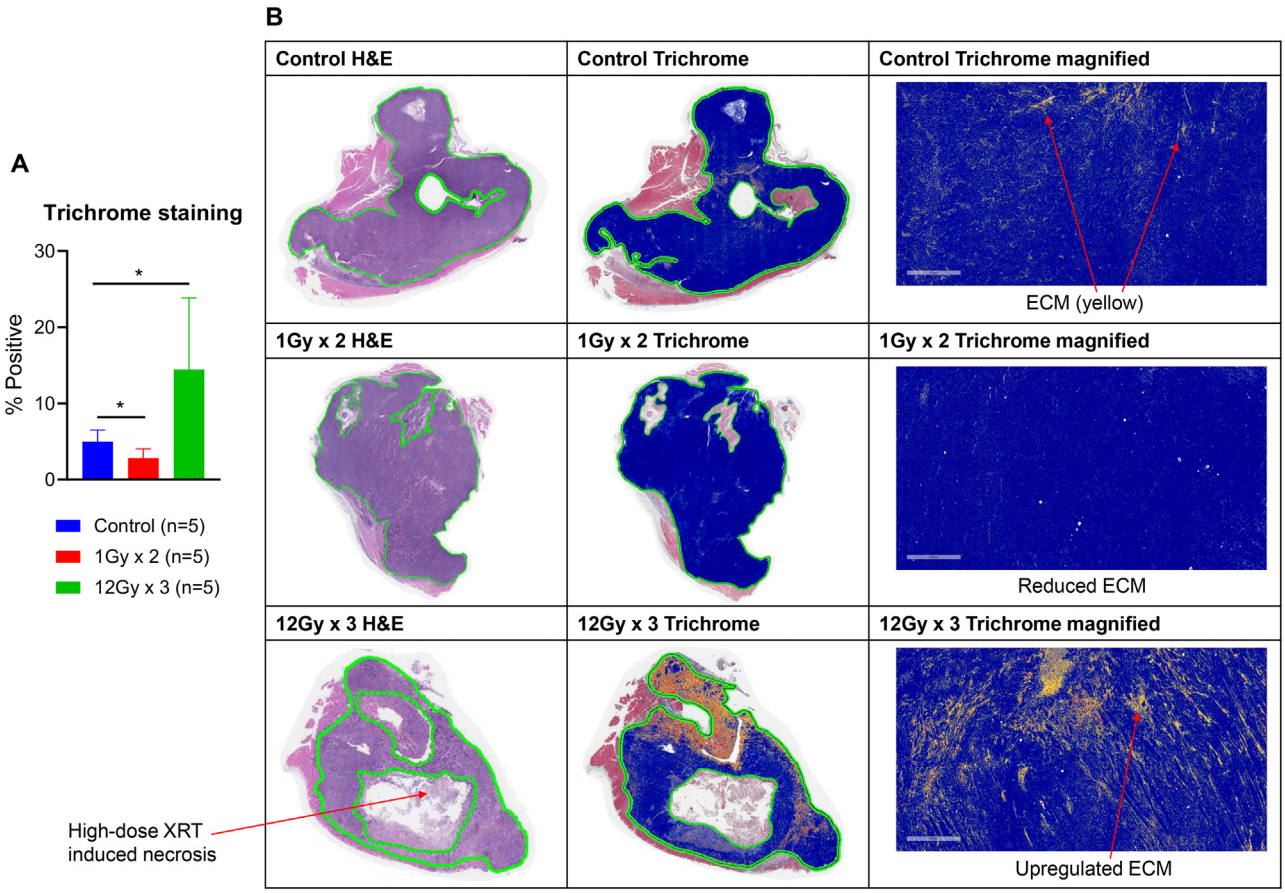

Figure 4 Low-dose radiation therapy downregulates the extracellular matrix in 344SQ-parental tumors depicted by Masson's trichrome staining for collagen fibers. A, Tumors were harvested 2 days after the last dose of low-dose radiation therapy and 4 days after the last dose of high-dose radiation therapy to conduct the staining. Percent stain positivity was reported for the control, 1 Gy × 2, and 12 Gy × 3 treatments (n = 5 mice per group). Groups were compared using Student's t tests. *$P \leq 0.05$. B, Left column: Representative hematoxylin and eosin stained images; middle column: Representative trichrome stained images; right column: Histochemical images shown at 5× magnification for the specified radiation therapy doses.

Discussion

Intratumoral pressure is an essential obstacle that must be addressed and overcome to improve intratumoral drug delivery and retention. Solving this issue would allow for intratumoral drugs to become more homogenously distributed throughout the tumor and, in turn, enhance antitumor responses.[21] The increased pressure present in cancer cells compared with normal tissue cells can be explained by interstitial fluid pressure, solid stress (SS), stiffness, and microarchitecture.[22] The interstitial fluid space is primarily held together by SS, which is directly correlated with multiple factors, including ECM (comprised of collagen and hyaluronan) and cancer-associated fibroblasts. Therefore, an increase in ECM results in an overall increase in intratumoral pressure. Additionally, the cross-linking of ECM is the primary cause of matrix stiffening, as well as changes in the matrix architecture.[22] The ECM not only increases intratumoral pressure, but also promotes tumor growth, cancer cell migration, and resistance to apoptosis.[23] Since radiation can be administered in conjunction with different intratumoral drugs used to treat cancer (eg, oncolytic viruses, NLRP3 agonists, STING agonists, antibodies, nanoparticles), assessing how radiation can reduce intratumoral pressure and help intratumoral drug delivery, as well as retention, is important.[24]

The direct delivery of anticancer therapies into tumors, particularly immunostimulatory agents, is a flourishing strategy to overcome resistance mechanisms for systemically administered immunotherapies and associated toxicities.[25-29] However, in practice, physical properties of tumors clearly also impose challenges to intratumoral delivery and deposition, even when the therapeutic agent is directly injected into the tumor.[26,29] Adjuvant interventions that can modulate the tumor's physical properties (stiffness, fibrosis status, composition of inhibitory stroma and ECM) to render the lesion more amenable to intratumoral injection have the potential to substantially augment the efficacy of these therapies.

To assess how different doses of radiation (1 Gy × 2, 5 Gy × 3, 8 Gy × 3, 12 Gy × 3, 20 Gy × 1) would affect intratumoral pressure in the 344SQ-P murine model, we measured intratumoral pressure 1, 3, 8, and 12 days after the last fraction of XRT using a compass computed tomography pressure transducer. Additionally, tumor growth was recorded to see the efficacy of the different radiation doses. We found that all groups significantly hampered tumor growth with 1 Gy × 2, 12 Gy × 3, and 20 Gy × 1 being the most significant. Moreover, 12 Gy × 3 controlled tumor growth better than 8 Gy × 3. In addition, 12 Gy × 3 and 1 Gy × 2 had similar effects on tumor control.

Low-dose XRT created an early window of low intratumoral pressure 1 to 3 days after XRT. A recent study showed that low-dose XRT modulates the tumor stroma and downregulates cancer-associated fibroblasts,[30] which causes the stroma to become more permeable and allows for effector immune cells (mainly natural killer and T cells) to infiltrate the TME. Once the natural killer and T cells infiltrate the stroma, immune-mediated killing begins. Additionally, TGF-β is reduced with low-dose XRT.[16] Although reduction of intratumoral pressure with low-dose XRT was attributed to modulation of the stroma and immune-mediated killing, high-dose XRT physically killed tumor cells. With more necrosis and space between tumor cells, intratumoral pressure dropped. Three fractions of 12 Gy produced a sustained window of low intratumoral pressure 3, 8, and 12 days after XRT. The effects of a single fraction of 20 Gy were different in that pressure dropped in the early (day 1) and late (day 12) timepoints after XRT.

To further examine the effect of different radiation regimens on intratumoral pressure, we followed the same experimental design as the first experiment. However, instead of the 344SQ-P cell line, we established tumors with an aggressive 344SQ-R cell line (Kras mutated, p53 deficient).[31] Similar to the previous experiment, all doses of radiation significantly controlled tumor growth, but there were differences among these experimental groups. In 344SQ-R, 3 fractions of 8 Gy controlled tumors similarly to 3 fractions of 12 Gy, but in the 344SQ-P model, 12 Gy proved to control tumor growth better than 8 Gy.

Another notable difference was that 2 fractions of 1 Gy underperformed the efficacy of 3 fractions of 12 Gy. This difference could be due to a more resilient inhibitory stroma associated with the 344SQ-R model, leading to reduced cluster of differentiation 4^+ and 8^+ tumor infiltrating lymphocytes.[32] Low-dose XRT once again created an early window of decreased intratumoral pressure 1, 3, and 5 days after the last fraction of XRT in 344SQ-R, and 3 fractions of 12 Gy only reduced intratumoral pressure 1 day after XRT (as opposed to the parental model with reduced pressure on days 3-12). Three fractions of 5 Gy and 8 Gy also only reduced pressure 1 day after XRT.

Extensive imaging was conducted to measure percent tumor fill after different doses of XRT 3 and 6 days after treatment. First, 100μL of iodinated contrast dye (Visipaque 320) was injected into the tumor with a syringe pump (Harvard Apparatus) at a rate of 5 cc per minute. Concurrently, live imaging was conducted using the Siemens Artis Q C-Arm. The mice were then transferred to the Bruker SkyScan 1276 for high resolution microCT imaging. Percent tumor fill was calculated from the images produced using the following formula: (Contrast volume/tumor volume) × 100. When intratumoral pressure was too high, the osmotic/oncotic pressure causing the contrast dye to reenter the capillaries could be seen. Two fractions of 1 Gy showed a significant increase in tumor fill 3 days after XRT, confirming the early window of low intratumoral pressure in the previous experiments. As the pressure lowered, the

contrast dye was more homogenously distributed around the TME. Moreover, 2 fractions of 1 Gy showed no significant increase in percent tumor fill 6 days after XRT, which is in line with the first set of experiments where intratumoral pressure was only reduced 1 to 3 days after 1 Gy × 2. Percent tumor fill of the 12 Gy group also followed the pressure readings from Figure 1B. Tumor fill was elevated 3 and 6 days after 12 Gy × 3, but was not statistically significant 6 days after XRT.

To investigate the mechanisms behind the increased tumor fill with 2 fractions of 1 Gy and 3 fractions of 12 Gy, a histopathologic evaluation was conducted using Masson's trichrome to stain for ECM, which consists mostly of collagen and hyaluronic acid (HA). Recent studies have shown that several drugs that target collagen and/or hyaluronic acid reduce interstitial fluid pressure, such as collagenase, PEGPH20 (targets HA), losartan (targets collagen and HA), and bevacizumab (targets vascular endothelial growth factor receptors).[32-35] When vascular endothelial growth factor receptors are inhibited, blood vessels are normalized and blood flow is improved.[35]

An initial analysis of the trichrome-stained slides showed a significant downregulation of ECM 2 days after low-dose XRT and an upregulation of ECM 4 days after high-dose XRT. The reduced ECM with low-dose XRT was as expected. As collagen is reduced in the interstitial space, SS is decreased and pressure is relieved from the tumor, enabling drugs to distribute intratumorally. Contrarily, the ECM was upregulated with 3 fractions of 12 Gy, most of which was observed to be deposited along the tumor periphery and the core presented with necrosis upon pathologic evaluation. One explanation of improved tumor fill with 12 Gy × 3 is that the upregulated peripheral ECM traps the intratumoral drugs inside and promotes retention. Overall, both doses of XRT (1 Gy × 2 and 12 Gy × 3) improved percent tumor fill; however, the underlying mechanisms are different.

Conclusions

These novel findings with optimized radiation therapy doses facilitate the delivery of intratumoral drugs and enhance their retention to maximize tumor killing. This is directly applicable to clinical settings where drugs have to be injected locally to avoid systemic toxicity and turn immunologically cold tumors into hot.

Supplementary materials

Supplementary material associated with this article can be found in the online version at doi:10.1016/j.adro.2022.101137.

References

1. Schmid P, Adams S, Rugo HS, et al. Atezolizumab and nab-paclitaxel in advanced triple-negative breast cancer. *N Engl J Med*. 2018;379:2108-2121.
2. Tawbi HA, Forsyth PA, Algazi A, et al. Combined nivolumab and ipilimumab in melanoma metastatic to the brain. *N Engl J Med*. 2018;379:722-730.
3. Demaria S, Golden EB, Formenti SC. Role of local radiation therapy in cancer immunotherapy. *JAMA Oncol*. 2015;1:1325-1332.
4. Formenti SC, Rudqvist NP, Golden E, et al. Radiotherapy induces responses of lung cancer to CTLA-4 blockade. *Nat Med*. 2018;24:1845-1851.
5. Golden EB, Chhabra A, Chachoua A, et al. Local radiotherapy and granulocyte-macrophage colony-stimulating factor to generate abscopal responses in patients with metastatic solid tumours: A proof-of-principle trial. *Lancet Oncol*. 2015;16:795-803.
6. Twyman-Saint Victor C, Rech AJ, Maity A, et al. Radiation and dual checkpoint blockade activate non-redundant immune mechanisms in cancer. *Nature*. 2015;520:373-377.
7. Amaria RN, Reddy SM, Tawbi HA, et al. Neoadjuvant immune checkpoint blockade in high-risk resectable melanoma. *Nat Med*. 2018;24:1649-1654.
8. Blank CU, Rozeman EA, Fanchi LF, et al. Neoadjuvant versus adjuvant ipilimumab plus nivolumab in macroscopic stage III melanoma. *Nat Med*. 2018;24:1655-1661.
9. Forde PM, Chaft JE, Smith KN, et al. Neoadjuvant PD-1 blockade in resectable lung cancer. *N Engl J Med*. 2018;378:1976-1986.
10. Huang AC, Orlowski RJ, Xu X, et al. A single dose of neoadjuvant PD-1 blockade predicts clinical outcomes in resectable melanoma. *Nat Med*. 2019;25:454-461.
11. Schalper KA, Rodriguez-Ruiz ME, Diez-Valle R, et al. Neoadjuvant nivolumab modifies the tumor immune microenvironment in resectable glioblastoma. *Nat Med*. 2019;25:470-476.
12. Hong WX, Haebe S, Lee AS, et al. Intratumoral immunotherapy for early-stage solid tumors. *Clin Cancer Res*. 2020;26:3091-3099.
13. Marabelle A, Tselikas L, de Baere T, Houot R. Intratumoral immunotherapy: Using the tumor as the remedy. *Ann Oncol*. 2017;28:xii33-xii43.
14. Ariffin AB, Forde PF, Jahangeer S, Soden DM, Hinchion J. Releasing pressure in tumors: What do we know so far and where do we go from here? A review. *Cancer Res*. 2014;74:2655-2662.
15. Heldin CH, Rubin K, Pietras K, Ostman A. High interstitial fluid pressure—An obstacle in cancer therapy. *Nat Rev Cancer*. 2004;4:806-813.
16. Barsoumian HB, Ramapriyan R, Younes AI, et al. Low-dose radiation treatment enhances systemic antitumor immune responses by overcoming the inhibitory stroma. *J Immunother Cancer*. 2020:8.
17. Znati CA, Rosenstein M, Boucher Y, Epperly MW, Bloomer WD, Jain RK. Effect of radiation on interstitial fluid pressure and oxygenation in a human tumor xenograft. *Cancer Res*. 1996;56:964-968.
18. Vanpouille-Box C, Alard A, Aryankalayil MJ, et al. DNA exonuclease TREX1 regulates radiotherapy-induced tumour immunogenicity. *Nat Commun*. 2017;8:15618.
19. Kang J, Demaria S, Formenti S. Current clinical trials testing the combination of immunotherapy with radiotherapy. *J Immunother Cancer*. 2016;4:51.
20. Carson FL. *Histotechnology: A Self-Instructional Text*. 2nd ed Chicago, IL: American Society for Clinical Pathology; 1997.
21. Jain RK. Physiological barriers to delivery of monoclonal antibodies and other macromolecules in tumors. *Cancer Res*. 1990;50:814s-819s.
22. Nia HT, Munn LL, Jain RK. Physical traits of cancer. *Science*. 2020:370.
23. Kim HG, Yu AR, Lee JJ, Lee YJ, Lim SM, Kim JS. Measurement of tumor pressure and strategies of imaging tumor pressure for radioimmunotherapy. *Nucl Med Mol Imaging*. 2019;53:235-241.

24. Baronzio G, Parmar G, Baronzio M. Overview of methods for overcoming hindrance to drug delivery to tumors, with special attention to tumor interstitial fluid. *Front Oncol*. 2015;5:165.
25. Qiao Y, Sheth R, Tam A. Image-guided intratumoral delivery of immunotherapeutics in gastrointestinal malignancies. *Dig Dis Interventions*. 2021;05:22-31.
26. Munoz NM, Williams M, Dixon K, et al. Influence of injection technique, drug formulation and tumor microenvironment on intratumoral immunotherapy delivery and efficacy. *J Immunother Cancer*. 2021;9.
27. Tselikas L, Champiat S, Sheth RA, et al. Interventional radiology for local immunotherapy in oncology. *Clin Cancer Res*. 2021;27:2698-2705.
28. Sheth R. Intratumoral and oncoviral immunotherapy. *Dig Dis Interventions*. 2021;5:050-054.
29. Sheth RA, Murthy R, Hong DS, et al. Assessment of image-guided intratumoral delivery of immunotherapeutics in patients with cancer. *JAMA Netw Open*. 2020;3: e207911.
30. He K, Barsoumian HB, Bertolet G, et al. Novel use of low-dose radiotherapy to modulate the tumor microenvironment of liver metastases. *Front Immunol*. 2021;12:812210.
31. Wang X, Schoenhals JE, Li A, et al. Suppression of type i ifn signaling in tumors mediates resistance to anti-pd-1 treatment that can be overcome by radiotherapy. *Cancer Res*. 2017;77: 839-850.
32. Chauhan VP, Martin JD, Liu H, et al. Angiotensin inhibition enhances drug delivery and potentiates chemotherapy by decompressing tumour blood vessels. *Nat Commun*. 2013;4:2516.
33. Provenzano PP, Cuevas C, Chang AE, Goel VK, Von Hoff DD, Hingorani SR. Enzymatic targeting of the stroma ablates physical barriers to treatment of pancreatic ductal adenocarcinoma. *Cancer Cell*. 2012;21:418-429.
34. Diop-Frimpong B, Chauhan VP, Krane S, Boucher Y, Jain RK. Losartan inhibits collagen I synthesis and improves the distribution and efficacy of nanotherapeutics in tumors. *Proc Natl Acad Sci U S A*. 2011;108:2909-2914.
35. Eikenes L, Bruland OS, Brekken C, de Lange Davies C. Collagenase increases the transcapillary pressure gradient and improves the uptake and distribution of monoclonal antibodies in human osteosarcoma xenografts. *Cancer Res*. 2004;64:4768-4773.